Electronic Supplementary Material (ESI) for Journal of Materials Chemistry C.

Supplementary Information for

Flexible and Multifunctional Composite Films Based on Rare Earth Phosphors as Broadband Thermal Emitters for High-Performance Passive Radiative Cooling

Ruiming Tan,[a] Wangyang Hu,[b] Xin Yao,[a]* Nan Lin,[b] Peng Xue,[c] Shiqing Xu,[a]* and Gongxun Bai[b]*

[a] College of Optical and Electronic Technology, China Jiliang University, Hangzhou 310018, China.

[b] Key Laboratory of Rare Earth Optoelectronic Materials and Devices of Zhejiang Province, China Jiliang University, Hangzhou 310018, China.

[c] Beijing Key Laboratory of Green Building Environment and Energy Saving Technology, Beijing University of Technology, Beijing 100124, China.

***Corresponding Author**

Email address: baigx@cjlu.edu.cn (G Bai), yaoxin_nk@126.com (X Yao), shiqingxu@cjlu.edu.cn (S Xu)

Supplementary Text:

Calculation of the cooling power intensity

In the following equation (1), $P_{rad}(T)$ is the power radiated outward by the radiator, P_{atm} is the atmospheric longwave radiation power absorbed by the radiator, and P_{solar} is the absorbed solar irradiance. P_{nonrad} refers to the non-radiative heat transfer power between the radiator and the surrounding environment, that is, conduction and convection.

$$P_{cooling}(T) = P_{rad}(T)-P_{solar}-P_{atm}-P_{nonrad} \quad (1)$$

Among them, D_{abs} is the absorption spectrum of the device, A_{atm} is the downward long-wave radiation flux spectrum of the atmosphere, I_{solar} is the solar spectrum, and the I_{bb} is the radiation power spectrum of the black-body at T. The h is the non-radiative heat transfer coefficient between the device and the surrounding environment, the T and T_{amb} are the device temperature, ambient air temperature, respectively.

These individual calculations are given by the following equations:[1,2]

$$P_{atm} = \int D_{RC}(\lambda)\, A_{atm}(\lambda) \quad (2)$$

$$P_{solar} = \int D_{RC}(\lambda)\, I_{sun}(\lambda) \quad (3)$$

$$P_{rad} = \int D_{RC}(\lambda)\, I_{bb}(\lambda) \quad (4)$$

$$P_{nonrad} = h(T-T_{amb}) \quad (5)$$

Among them, D_{RC} is the absorption spectrum of the device, A_{atm} is the downward long-wave radiation flux spectrum of the atmosphere, I_{sun} is the solar spectrum, and the $I_{bb} = \frac{2hc^2}{\lambda^5(e^{\frac{hc}{\lambda KT}}-1)}$ is the radiation power spectrum of the black-body at T. The h is the non-radiative heat transfer coefficient between the device and the surrounding environment, the T and T_{amb} are the device temperature, ambient air temperature, respectively.

Calculation of the average solar reflectivity and thermal emissivity

The solar reflectance (**R_{solar}**) and mid-infrared band thermal emissivity (**ε_{IR}**). The selective longwave infrared (**LWIR**) emittance (**ε_{LWIR}**) measured by experiment, their average value can be calculated by the following equations:[3]

$$\overline{\mathbf{R}}_{\mathbf{solar}} = \frac{\int_{0.3\ \mu m}^{2.5\ \mu m} I_{AM1.5}(\lambda)R(\lambda)d(\lambda)}{\int_{0.3\ \mu m}^{2.5\ \mu m} I_{AM1.5}(\lambda)d(\lambda)} \tag{6}$$

And

$$\overline{\boldsymbol{\varepsilon}}_{\mathbf{IR}} = \frac{\int_{2.5\mu m}^{25\ \mu m} I_{bb}(\lambda,T)\varepsilon(\lambda)d(\lambda)}{\int_{2.5\mu m}^{25\ \mu m} I_{bb}(\lambda,T)d(\lambda)} \tag{7}$$

$$\overline{\boldsymbol{\varepsilon}}_{\mathbf{LWIR}} = \frac{\int_{8\ \mu m}^{13\ \mu m} I_{bb}(\lambda,T)\varepsilon(\lambda)d(\lambda)}{\int_{8\ \mu m}^{13\ \mu m} I_{bb}(\lambda,T)d(\lambda)} \tag{8}$$

The $I_{AM1.5}(\lambda)$ is the AM 1.5 global standard solar intensity and R(λ) is the solar reflectivity of radiative cooler at wavelength λ. $I_{bb}(\lambda,T)$ is the radiation of a blackbody at a temperature of T and a wavelength of λ.

Supplementary Figures:

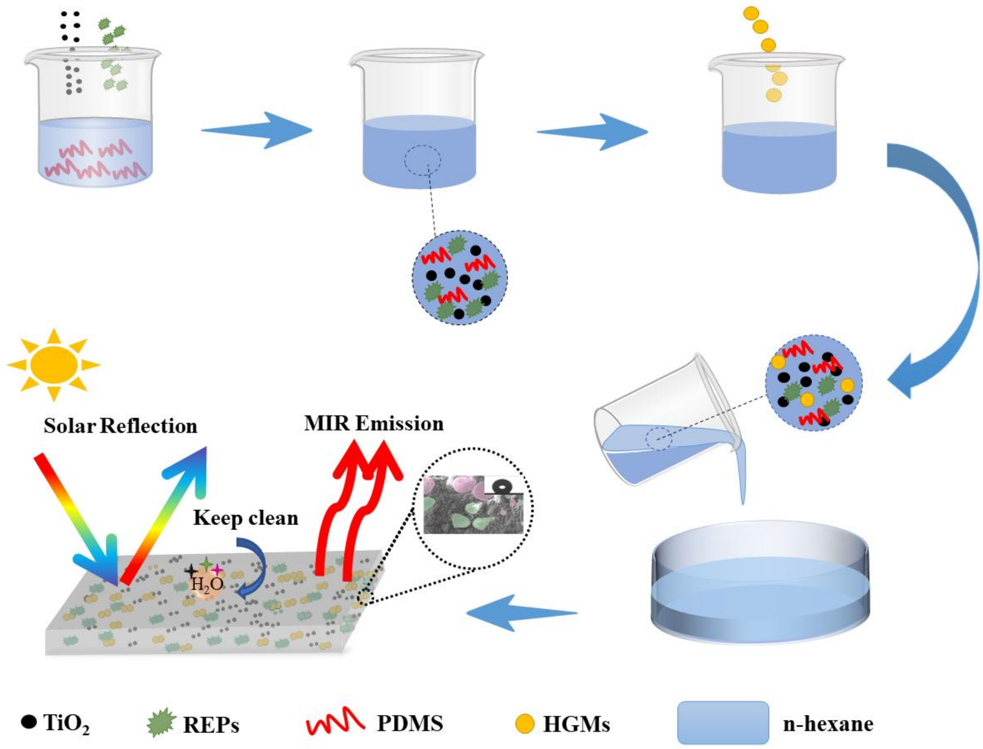

Fig. S1 Diagram of the fabrication process of the SA film and white film by stirring, mixing and drying.

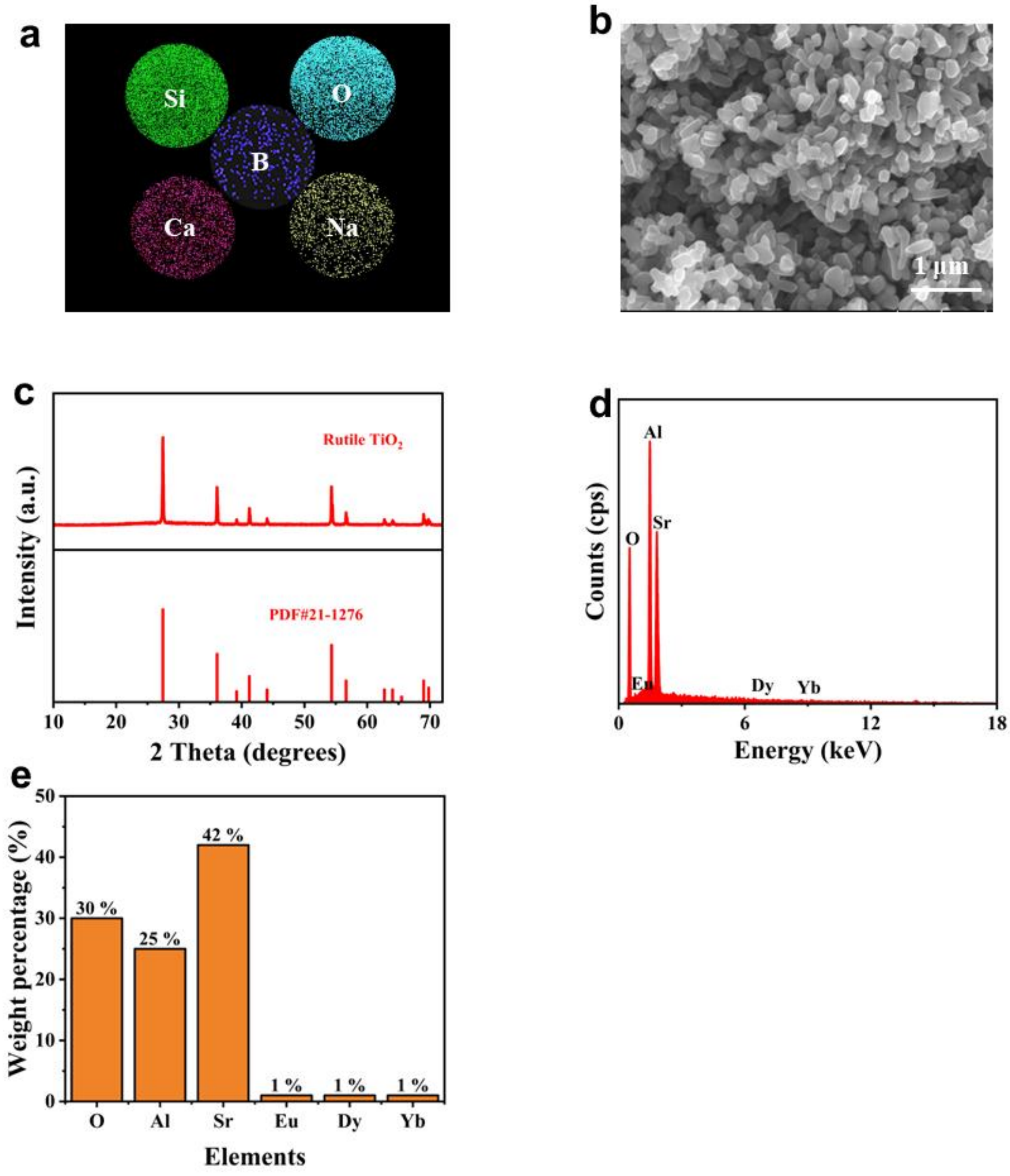

Fig. S2 Microstructures and chemical properties of materials. (a) The EDS elemental mappings of Si, O, Na, Ca and B in HGMs. (b) The SEM images of TiO_2 nanoparticles. (c) The XRD spectrum of TiO_2 nanoparticles. (d, e) The EDS elemental analysis of REPs.

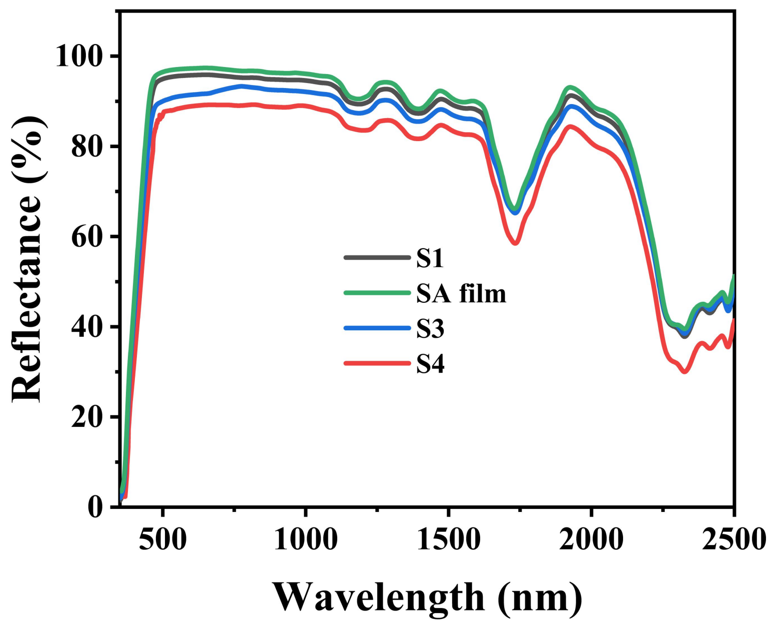

Fig. S3 The reflectance of composite films with corresponding mass ratio in Table S1.

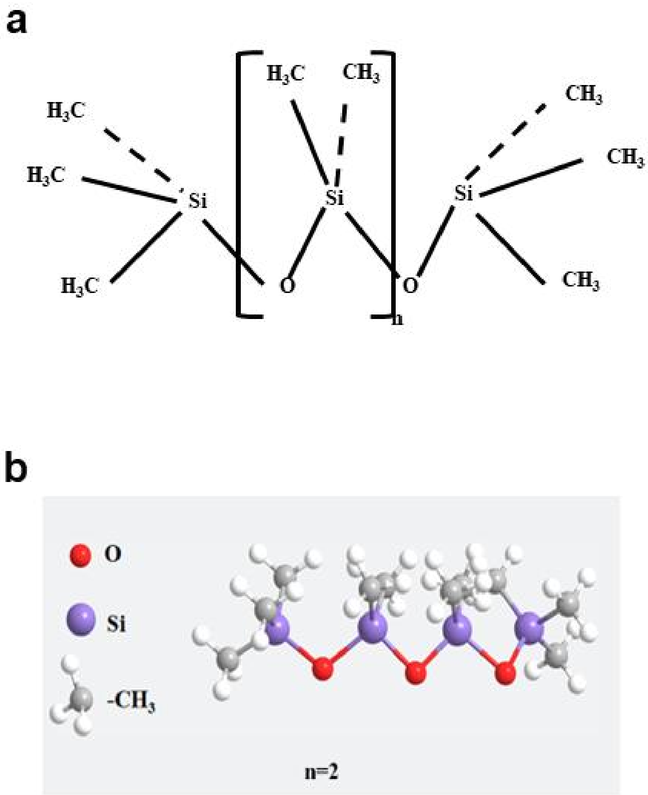

Fig. S4 Physicochemical information of the PDMS. (a) Chemical structure of the PDMS. (b) The three-dimensional structure of the PDMS (n = 2).

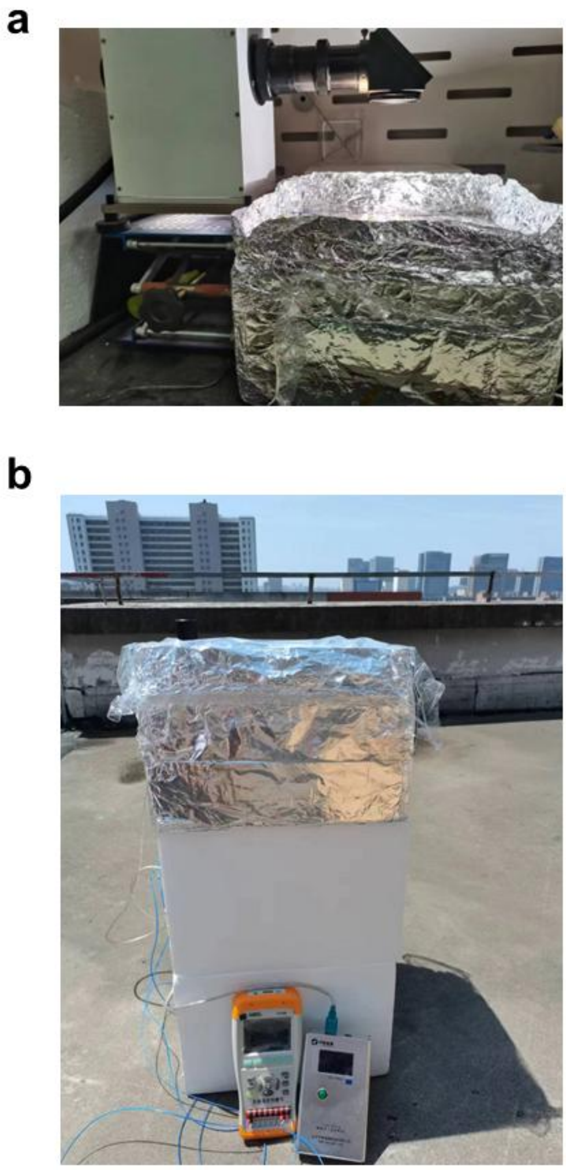

Fig. S5 The actual indoor and outdoor cooling devices. (a) The actual indoor cooling device. (b) The actual outdoor cooling device.

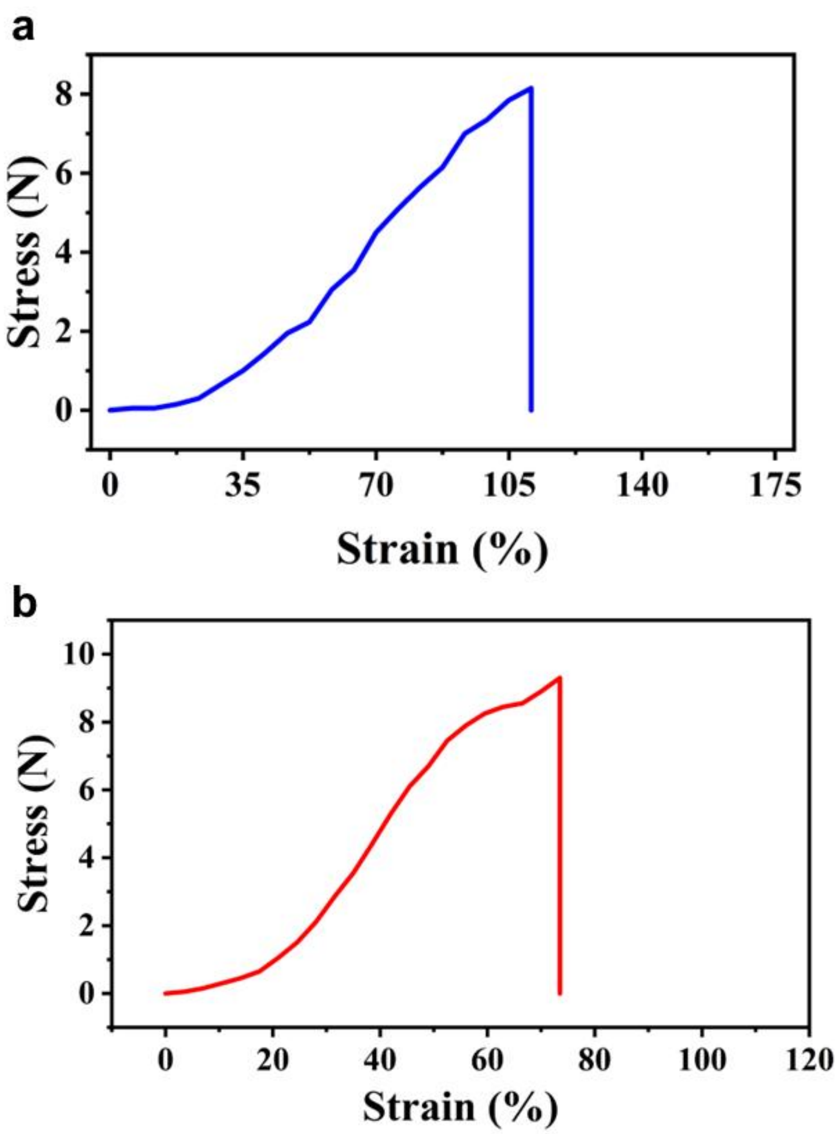

Fig. S6 Stress-strain curves of SA films of different thicknesses. (a) Stress-strain curve for SA film of 410 μm thickness. (b) Stress-strain curve for SA film of 510 μm thickness.

Table S1. The mass ratios of PDMS, TiO_2, HGMs, and REPs in the our composite film.

Samples \ Compositions	PDMS	TiO_2	HGMs	REPs
S1	60 %	26 %	5 %	9 %
SA film	60 %	23 %	5 %	12 %
S3	60 %	20 %	5 %	15 %
S4	60 %	17 %	5 %	18 %

Table S2. The reflectances of the white film and SA film in visible (0.4 to 0.78 µm; $\mathbf{R_{VIS}}$) and near shortwave infrared (NSWIR) (0.78 to 2.5 µm; $\mathbf{R_{NSWIR}}$), and the broadband solar reflectance (0.3 to 2.5 µm; $\mathbf{R_{solar}}$) and the longwave infrared (LWIR) emittance (2.5 to 25 µm; $\boldsymbol{\varepsilon_{LWIR}}$), and the selective infrared (IR) emittance (8 to 13 µm; $\boldsymbol{\varepsilon_{IR}}$).

Samples	**White film**	**SA film**
$\mathbf{R_{VIS}}$	0.903	0.938
$\mathbf{R_{NSWIR}}$	0.894	0.911
Rsolar	0.881	0.903
$\boldsymbol{\varepsilon_{LWIR}}$	0.945	0.953
$\boldsymbol{\varepsilon_{IR}}$	0.950	0.955

Table S3. The comparison of cooling performance with other reported results involves **reflectance** (0.3 to 2.5 μm), **emittance** (2.5 to 25 μm), and the temperature differences between the ambient environment and the radiative coolers (**ΔT**).

Samples	Reflectance	Emittance	ΔT (°C)	Ref.
Fluorescent coatings	0.898	0.900	7	[1]
Polymethyl methacrylate films	0.850	0.984	8.1	[4]
Shish-kebab superstructure films	0.830	0.870	8.2	[5]
Cellulose-based fabric	0.917	0.900	7.5	[6]
Self-Cleaning polymer composites	0.921	0.75	7.8	[7]
Scalable-manufactured dual-layer coating	0.880	0.920	3.6	[8]
Double-layer coating	0.90	0.90	/	[9]
A tandem radiative/evaporative cooler	0.930	0.800	10	[10]
SA film	**0.903**	**0.953**	**11.4**	**This work**

REFERENCES

1. X. Xue, M. Qiu, Y. Li, Q. M. Zhang, S. Li, Z. Yang, C. Feng, W. Zhang, J. Dai, D. Lei, W. Jin, L. Xu, T. Zhang, J. Qin, H. Wang and S. Fan, *Adv. Mater.*, 2020, **32**, 1906751.

2. J. Li, Y. Fu, J. Zhou, K. Yao, X. Ma, S. Gao, Z. Wang, J.-G. Dai, D. Lei and X. Yu, *Sci. Adv.*, 2023, **9**, eadg1837.

3. M. Yang, H. Zhong, T. Li, B. Wu, Z. Wang and D. Sun, *ACS Nano*, 2023, **17**, 1693–1700.

4. G. Qi, X. Tan, Y. Tu, X. Yang, Y. Qiao, Y. Wang, J. Geng, S. Yao and X. Chen, *ACS Appl. Mater. Interfaces*, 2022, **14**, 31277–31284.

5. X. Liu, Y. Li, Y. Pan, Z. Zhou, Z. Zhai, C. Liu and C. Shen, *ACS Appl. Mater. Interfaces*, 2023, **15**, 17188-17194.

6. Y. Zhang, W. Zhu, C. Zhang, J. Peoples, X. Li, A. L. Felicelli, X. Shan, D. M. Warsinger, T. Borca-Tasciuc, X. Ruan and T. Li, *Nano Lett.*, 2022, **22**, 2618–2626.

7. K. Zhou, X. Yan, S. J. Oh, G. Padilla-Rivera, H. A. Kim, D. M. Cropek, N. Miljkovic and L. Cai, *Nano Lett.*, 2023, **23**, 3669–3677.

8. S. Wang, Y. Wang, Y. Zou, G. Chen, J. Ouyang, D. Jia and Y. Zhou, *ACS Appl. Mater. Interfaces*, 2021, **13**, 21888–21897.

9. Z. Huang and X. Ruan, *International Journal of Heat and Mass Transfer*, 2017, **104**, 890–896.

10. J. Li, X. Wang, D. Liang, N. Xu, B. Zhu, W. Li, P. Yao, Y. Jiang, X. Min, Z. Huang, S. Zhu, S. Fan and J. Zhu, *Sci. Adv.*, 2022, **8**, eabq0411.